PORPHYRINE/SILVER NANOPARTICLES BASED PHOTOACTIVE ANTIBACTERIAL COATINGS

Nikoleta Philipova[1], Nikolay Georgiev[2], Damyan Ganchev[3], Ivo Lalov[4], Rayna Bryaskova[1]

[1]*Department of Polymer Engineering*
University of Chemical Technology and Metallurgy
8 Kliment Ohridski blvd., Sofia, 1756, Bulgaria
[2]*Department of Organic Synthesis*
University of Chemical Technology and Metallurgy
8 Kliment Ohridski blvd., Sofia, 1756, Bulgaria
[3]*Department of Machine Elements and Non-metal Constructions*
Technical University, Sofia, Bulgaria
[4]*Department of Biotechnology*
University of Chemical Technology and Metallurgy
8 Kliment Ohridski blvd., Sofia, 1756, Bulgaria
E-mail: rbryaskova@uctm.edu

Received 06 December 2022
Accepted 29 December 2022

ABSTRACT

A novel amino-modified protoporphyrin IX with included silver nanoparticles (PPIX-ED/AgNPs) complex was synthesized and used as a last layer for preparation of photoactive antibacterial coatings. The obtained PPIX-ED/AgNPs complex was appropriately analyzed using various spectroscopic methods such as fluorescence analysis and infrared spectroscopy (ATR-FTIR). The size and morphology of the synthesized PPIX-ED/AgNPs complex were analyzed by Transmission electron microscopy (TEM) and dynamic light scattering (DLS). Then, the photoactive antibacterial coatings were obtained by deep coating procedure as the last layer consists of PPIX-ED/AgNPs complex, which is expected to possess strong antibacterial activity. The EDX-SEM analysis was employed to prove the deposition of the layers and nanoindentation analysis was used to determine their mechanical properties. The antibacterial properties of the photoactive coatings against G. negative E. coli and G. positive B. Subtilis were determined using disk diffusion method (DDM).

Keywords: antibacterial coatings, photosensitizer, silver nanoparticles.

INTRODUCTION

Nowadays, the development of novel and more effective antibacterial coatings for the antimicrobial treatment of resistant bacteria are of great importance, since antibacterial resistance is emerging as a global problem and poses a risk to human health. Among the new strategies, two main approaches are under intensive investigation which explores the application of metal nanoparticles (MeNPs) or the use of light-activated compounds called photosensitizers [1]. Among MeNPs, silver nanoparticles (AgNPs) have the most successful antibacterial activity since they destroy effectively bacterial wall and disturb intracellular balance [2]. It is well known that silver is able to kill both Gram-negative and Gram-positive pathogens due to a complex mechanism of action, and it is more difficult for bacteria to develop a resistance to silver in comparison to conventional used means [3, 4]. Materials with included AgNPs are classified as releasing because of the way they work [5]. Another alternative approach to preparing effective antibacterial coatings is based on the use of photosensitizers, which with a combination of visible light and oxygen produce highly reactive oxygen species (ROS) that react with a variety of substrates causing damage to cell and their inactivation [6]. In this way, photodynamic inactivation (PDI) of microorganisms occurs regardless of antibiotic resistance. Some physical

methods were developed to incorporate different photosensitizers into surfaces [7], however, the chemical methods by the formation of covalent bonds between a photosensitizer and the surface are the preferred approach since it can increase the stability and prevent it from leaching into the environment [8]. Among the photosensitizers, porphyrin is well known for its high photo and antibacterial activity. Several porphyrin-based compounds have demonstrated the photosensitization of pathogenic microorganisms upon visible light irradiation [9]. Different photobactericidal materials have been developed including porphyrin as grafting porphyrin-based compounds onto nylon fibers [10], alkylated cellulose [11], poly(methylmethacrylate) (PMMA) [1, 12] or covalently bonded to polyethylene terephthalate (PET) [13].

Here, we report on the preparation of photoactive antibacterial coatings on stainless steel (SS) as the last layer is employed covalently bonded to the substrate complex of amino-modified protoporphyrin IX with included silver nanoparticles (PPIX-ED/AgNPs). In this way, porphyrin molecules act as a light absorber with an antimicrobial response and silver nanoparticles except that enhanced this response protect the porphyrin against photobleaching and for conservation of energy by suppression of porphyrin luminescence [1].

EXPERIMENTAL

Materials

Protoporphyrin IX (PPIX) (Sigma-Aldrich), N-Hydroxysuccinimide (NHS), and 1-(3-dimethylaminopropyl)-3-ethyl carbodiimide hydrochloride, 98 % (EDC) (Alfa Aesar) were used without further purification. Stainless steel (SS) 316 was used as a substrate. Poly(N-methacryloyl 3,4-dihydroxy-L-phenylalanine methyl ester)-b-poly(2-methacrylox yethyltrimethylammonium chloride) (P(mDOPA)-co-P(DMAEMA+) copolymer [14],poly(N-methacryloyl 3,4-dihydroxy-L-phenylalanine methyl ester) (P(mDOPA)) [15], and a silver loaded (Pox(mDOPA)/PAH) cross-linked nanogel [16] were prepared as reported in the mentioned publications [14 - 16].

Synthesis of amino-modified protoporphyrin/silver complex (PPIX-ED/AgNps)

The amino derivative of PPIX (PPIX-ED) was synthesized according to [10]. Then PPIX-ED (0.1 g, 0.1546 mmol) was dispersed in 15 mL acetonitrile for 24 h at room temperature. After 24 h, $AgNO_3$ (0.024 g, 0.1418 mmol) dissolved in 1 mL acetonitrile was added to the reaction mixture at room temperature. Thus, the reaction mixture was allowed to stir for 3 h. $NaBH_4$ solution (0.0316 g, 0.8341 mmol in 2 mL CH_3OH) was then slowly added to the reaction flask and kept in an ice bath. The resulting mixture was stirred for 4 h at room temperature. The product was washed with acetonitrile (10 mL) and centrifuged. Then 10 mL H_2O was added and the aqueous dispersed PPIX-ED/AgNPs complex was obtained.

Preparation of the antibacterial polymer coatings on SS substrate

SS substrates (1.0 cm x 1.0 cm) were cleaned and degreased by washing for 2 minutes with ethanol and acetone, respectively, and dried with nitrogen. The coatings were prepared at room temperature by deep coating procedure as the substrates were successively dipped for 15 min, and rinsed in deionized water for 5 min in the following solutions: 1) P(DOPA)-*co*-P(DMAEMA$^+$) (2 g L^{-1}, pH 7); 2) Pox(mDOPA)/PAH nanogel (1 g L^{-1}) and 3) PPIX-ED/AgNPs complex. The final coatings were allowed to dry at room temperature.

Characterizations

ATR FT-IR spectra were recorded using Agilent Cary 600 equipment. Transmission electron microscopy (TEM) observations were carried out with an HR STEM JEOL JEM 2100 instrument. Samples were prepared by deposition of a droplet of the aqueous PPID-ED/AgNPs solution onto a carbon-coated copper TEM grid and allowed to evaporate for 2 h. SEM-EDX spectra were recorded on SEM Lyra, Tescan with Quantax EDS detector - Bruker. Dynamic light scattering (DLS) measurements were performed using a Brookhaven instrument (NanoBrook 90Plus) with ZetaPlus Particle Sizing Software Version 5.23. Nanomechanical analyses were performed using Universal Nanomechanical Tester (UNMT, Bruker), equipped with Nanoindenter & Atomic Force Microscopy (AFM, Ambios Technology). For each specimen, 48 nanoindentations were made with force applied to 50 mN. The 70 nm diamond tip Berkovich indenter was used to perform the tests and specialized software to calculate the hardness and the modulus of elasticity of the specimens using the Oliver

Pharr method. All nanoindentation tests were performed at a constant temperature of 20°C. The inhibition zones of the tested samples were measured using Image-Pro Plus v 7.0 (Media Cybernetics, USA) [17]. Spatial and aspect ratio calibration of the images was done using the real dimensions of the SS substrates. After that two perpendicular lines were drawn through the center of the SS substrates. The Line Profile Analysis tool was used to measure the intensity values of the image through those lines. Values measured correspond to the optical density. Line length is measured between the points of abrupt optical density change. The inhibition zone is averaged from the lengths of the two perpendicular lines.

Antibacterial activity

The antibacterial activity of PPIX-ED/AgNps complex and P(DOPA)-*co*-P(DMAEMA$^+$)/Pox(mDOPA)/PAH/PPIX-ED/AgNPs coatings against Gram-negative bacteria *E. coli* NBIMCC K12407 and Gram-positive bacteria *B. subtilis* NBIMCC 3562 was tested by disk-diffusion method (DDM), modified by using a light source, which was necessary to ensure the photodynamic activity of the coatings. For PPIX-ED/AgNps complex, antibacterial test was performed by using disks from chromatographic paper (d = 6 mm), which were impregnated with 5 µL of the solutions and for the coatings, test was performed using SS substrate (1x1 cm). In this procedure, agar plates were inoculated with 0.2 mL standardized inoculum (10^7 cells. mL^{-1}) of the test microorganism. The samples were sterilized by UV irradiation and placed on the agar surface. The Petri dishes were illuminated using a 300 W spotlight (wavelength from 380 nm to 750 nm) and incubated under suitable conditions (30°C for *B. subtilis* and 37°C for *E. coli*) for 24 hours. Then the diameters of inhibition growth zones were measured. The antibacterial activity of neat SS substrate as a control sample was also tested under the same conditions.

RESULTS AND DISCUSSION

Photoactive antibacterial coatings were prepared as described in our previous investigations [18, 19], as the last layer consists of novel synthesized amino-modified protoporphyrin IX with included silver nanoparticles (PPIX-ED/AgNPs) thus forming coatings that possess strong antibacterial activity against G. positive and G. negative strains. To achieve this, we combine the photodynamic properties of protoporphyrin IX which is well-known photoactive photosensitizer with the antimicrobial activity of silver nanoparticles, thus expecting a strong antimicrobial effect arising from the interaction of AgNPs and PPIX-ED. Initially, chemical modification of PPIX to an ethylene diamino derivative of PPIX was performed. It is known that the free amine group of the ligand could be employed to anchor metal nanoparticles [20, 21]. Therefore, the amine groups of PPIX-ED were used for the encapsulation of AgNPs. The synthesis of PPIX-ED/AgNPs complex was performed using $AgNO_3$ as a precursor of silver in the presence of PPIX-ED and $NaBH_4$ as a reducing agent according to scheme 1.

To confirm that the chemical modification of PPIX does not affect its properties a fluorescent analysis of

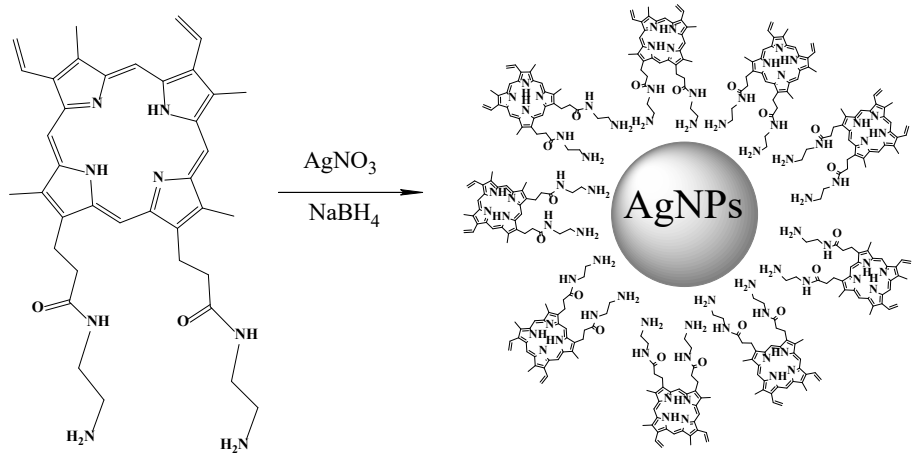

Scheme 1. Strategy for preparation of PPIX-ED/AgNPs complex.

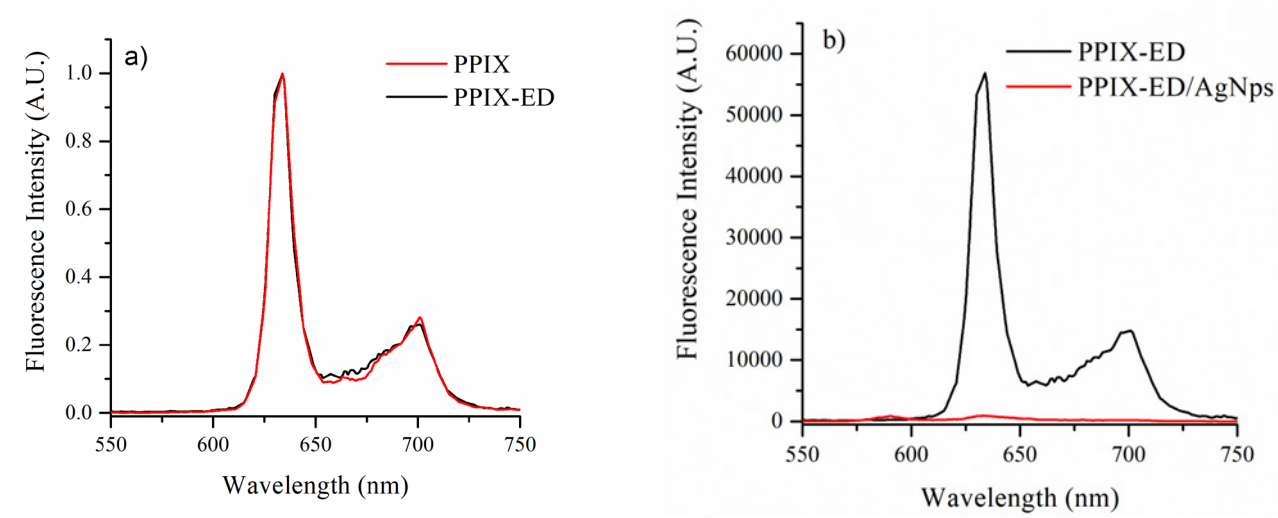

Fig. 1. Fluorescent spectra of a) - PPIX and PPIX-ED; b) - Fluorescent spectra of PPIX, PPIX-ED, and PPIX-ED/AgNPs.

the fluorescent emission of amino-modified PPIX-ED and PPIX was performed and their spectra were compared. It was established that the introduction of the ethylenediamine part in PPIX did not affect the conjugated fluorophoric system and both compounds showed the same fluorescent spectra (Fig. 1(a)). These results clearly showed that the photophysical properties of PPIX remain unchanged after ethylene diamine modification.

However, when PPIX-ED/AgNPs complex was analyzed, fluorescent emission was completely quenched. This could be attributed to an energy transfer from the fluorophore excited state to the neighbor metal nanoparticles. This result confirms the formation of PPIX-ED/AgNPs complex. Similar observations were also observed by Lyutakov et al., where the transfer of tetraphenylporphine (TPP) excited state on AgNPs was demonstrated and confirms the mutual coupling [1].

The FT-IR spectrum of PPIX-ED/AgNPs also demonstrated the formation of PPIX-ED/AgNPs complex as a shift of 20 cm^{-1} compared to the amino-modified PPIX-ED in the N-H stretching region (3280 cm^{-1}) was observed (Fig. 2). The shift in the N-H stretching frequency is probably caused by electrostatic interactions between NH_2 groups and the silver nanoparticle as reported by Natarajan et al. [22]. The characteristic peaks for PPIX-ED structure were also presented in the spectrum: 2898 cm^{-1} for vas (–CH_2–); 2858 cm^{-1} for vs(–CH_2–); 1619 cm^{-1} for ν (C=O) of –CONH– (Amide I band) and 1530 cm^{-1} for δ(N-H) of –CONH– (Amide II band).

Further, the size and morphology of the obtained PPIX-ED/AgNPs complex were determined by TEM analysis (Fig. 3). Well-defined AgNPs with an average size of 10 nm were obtained, which were uniformly distributed into PPIX-ED matrix (Figs. 3(a), 3(b)). The selected area electron diffraction (SAED) analysis demonstrated the crystalline nature of obtained AgNPs by appearing of all characteristic diffraction rings, which correspond to (111), (200), (220), and (311) reflections of the fcc (face-centered cubic) structure of silver (Fig. 3(c)). The DLS analysis also confirms the formation of nanoparticles with an average hydrodynamic diameter (Dh) of 50 nm at relatively high polydispersity.

Further, the photoactive coatings were prepared by sequential deposition on stainless steel (SS) substrate of the following components as a first layer was employed polycationic copolymer on the base of P(mDOPA)-co-P($DMAEMA^+$), used as a universal primer, as a second layer was used Pox(mDOPA)/PAH) nanogel decorated with quinone groups, which permit the covalent grafting of the PPIX-ED/AgNPs complex, and as the last layer was applied the synthesized PPIX-ED/AgNPs complex. The formation of the coating was demonstrated by using EDX-SEM analysis, as the elemental mapping showed uniformly distributed carbon (C), oxygen (O), nitrogen (N), and silver (Ag) on the SS substrate (Fig. 4(a)). The performed EDX-SEM analysis in a point indicated high silver content

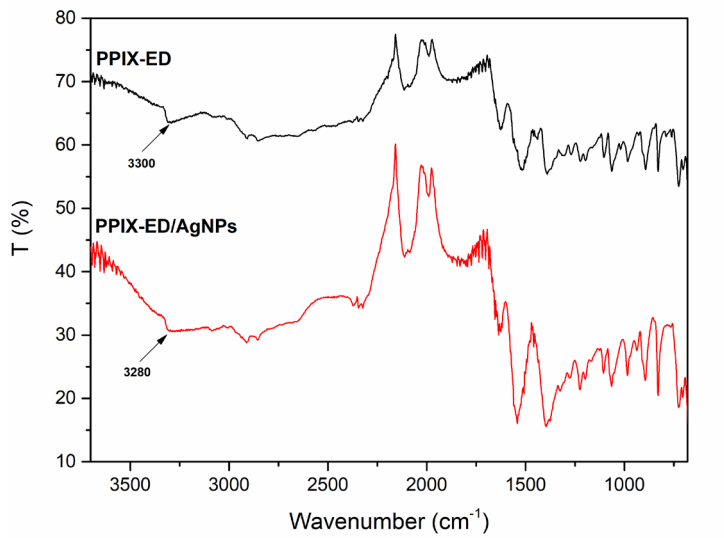

Fig. 2. ATR-FTIR spectra of amino-modified PPIX-ED and PPIX-ED/AgNPs complex.

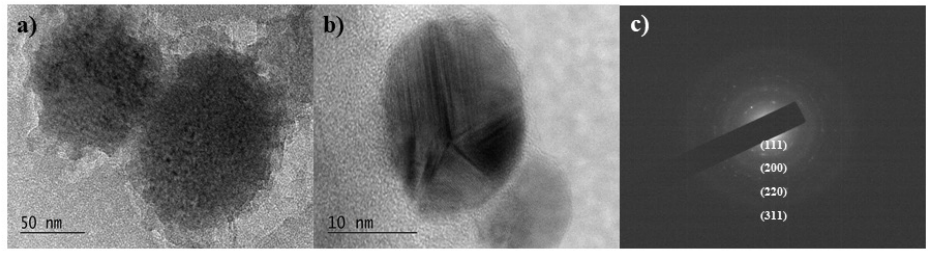

Fig. 3. a-b) - TEM analysis of PPIX-ED/AgNPs complex; c) - SAED of PPIX-ED/AgNPs complex.

of 7.73 at. % as well as the presence of C - 16.2 at. %, N - 15.6 at. % and O - 6.2 at. %, which are derived from the PPIX-ED component of the complex (Fig. 4(b)).

The mechanical properties of the coatings were obtained by using the nanoindentation method, which allows simultaneous evaluation of hardness (H) and elastic modulus (E) as a function of contact depth (hc) at a micron or sub-micron scale. The linear decrease of H and E values with increased contact depth was observed and this can be explained by a magnification of second-order displacement gradients when using a Berkovich type indentor [23].

The obtained average values of H and E for the coating on SS substrate were 1.64 GPa and 108.5 GPa respectively, which is indicative of the very good mechanical properties of the coatings (Fig. 5).

Further, the antibacterial properties of the obtained photoactive antibacterial coatings were determined, as initially, the antibacterial activity of the PPIX-ED/AgNPs complex by DDM was estimated against G. positive *B. subtilis* and G. negative *E. coli*. It was established that the synthesized complex possesses strong antibacterial activity against both strains and inhibition zones in the range of 12.0 - 12.4 mm was measured. Then the antibacterial activity of the coatings was tested against G. positive *B. subtilis* and G. negative *E. coli*. The strong antibacterial activity by the appearance of an inhibition zone of 14.5mm for *B. subtilis* and 17.5 mm for *E. coli* was detected in comparison to the neat SS substrate, where no inhibition zone was observed. (Fig. 6).

Higher antibacterial activity was observed against G. negative *E. coli* in comparison to G. positive *B. subtilis* which is due to the difference in their membrane structure. The results obtained demonstrated the potential of the prepared coating as a power antibacterial coating with long-term activity.

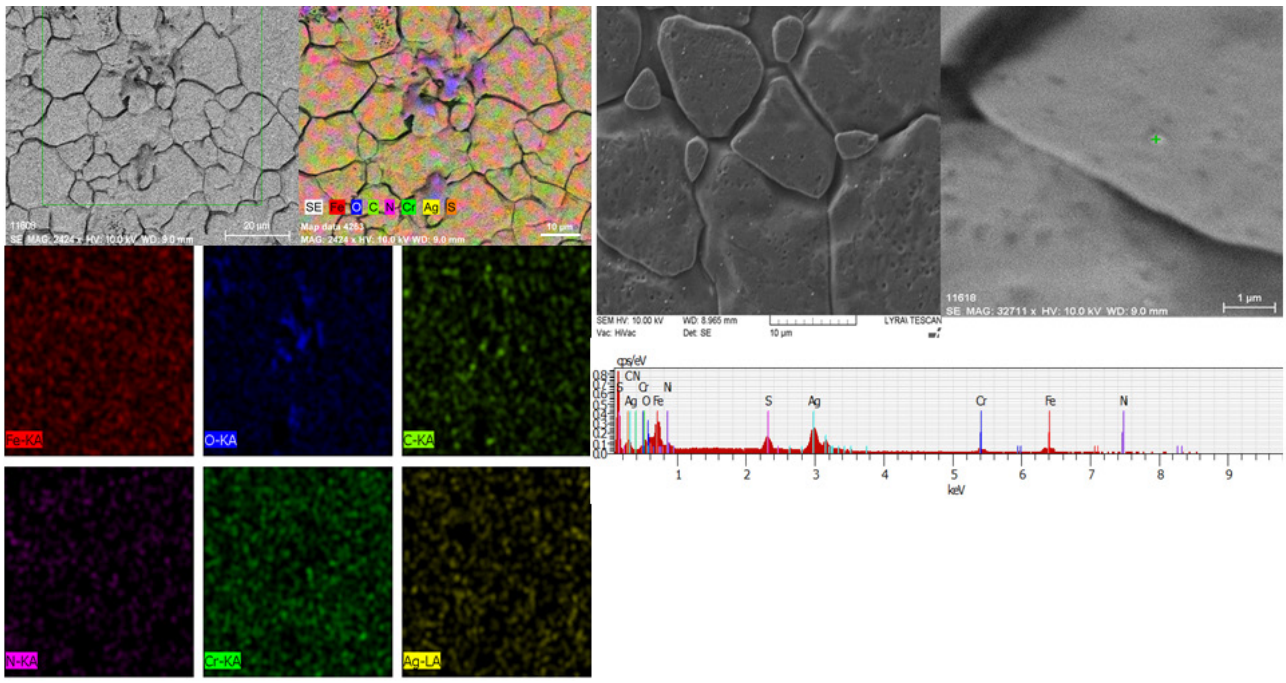

Fig. 4. EDX-SEM analysis of P(mDOPA)-*co*-P(DMAEMA$^+$)/Pox(mDOPA)/PAH/PPIX-ED/AgNPs coating on SS substrate.

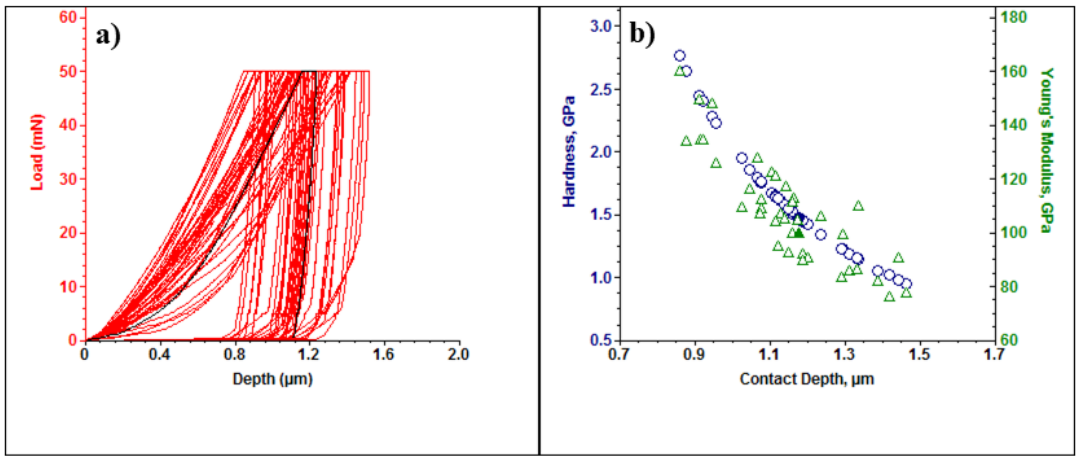

Fig. 5. a) - Nanoindentation curves; b) - hardness (H) and elastic modulus of light-activated coatings.

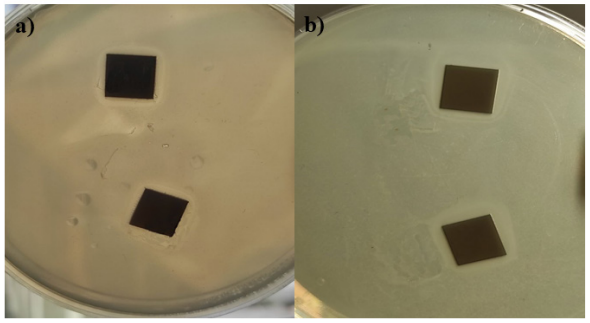

Fig. 6. Antibacterial activity of photoactive antibacterial coatings against: a) - *B. subtilis* and b) - *E.coli*.

CONCLUSIONS

Photoactive antibacterial coatings on SS were prepared using PPIX-ED/AgNPs complex as the last layer, which possesses strong antibacterial activity due to the combination of photodynamic properties of the PPIX photosensitizer used and AgNPs included in the complex. The obtained PPIX-ED/AgNPs complex was confirmed by fluorescent analysis and FTIR spectroscopy. The morphology and the size of PPIX-ED/AgNPs complex were estimated by TEM and DLS analysis. Then a photoactive antibacterial coating was obtained by the deep-coating procedure. The performed EDX-SEM analysis proved the successful deposition of the layers by the presence of all characteristic elements derived from the coating. The performed nanoindentation analysis demonstrated that the obtained coatings possess very good mechanical properties. Finally, strong antibacterial activity was estimated against G. negative and G. Positive strains. The results obtained showed that the obtained photoactive antibacterial coating has a high potential in many fields of industry.

Acknowledgements

This work was supported by the National Science Fund of Bulgaria (project no. KP-06-H29/5).

REFERENCES

1. O. Lyutakov, O. Hejna, A. Solovyev, Y. Kalachyova, V. Svorcik, Polymethylmethacrylate doped with porphyrin and silver nanoparticles as light-activated antimicrobial material, RSC advances, 4, 2014, 50624-50630.
2. J.S. Kim, E. Kuk, K.N. Yu, J.H. Kim, S.J. Park, H.J. Lee, S.H. Kim, Y.K. Park, C.Y. Hwang, Y.K. Kim, Y.S. Lee, D.H. Jeong and M.H. Cho, Antimicrobial effects of silver nanoparticles, Nanomedicine: Nanotechnology, Biology and Medicine, 3, 2007, 95-10.
3. R. Bryaskova, D. Pencheva, S. Nikolov, T. Kantardjiev, Synthesis and comparative study on the antimicrobial activity of hybrid materials based on silver nanoparticles (AgNps) stabilized by polyvinylpyrrolidone (PVP), Journal of chemical biology, 4, 2011, 185-191.
4. R. Bryaskova, D. Pencheva, G.M. Kale, U. Lad, T. Kantardjiev, Synthesis, characterization and antibacterial activity of PVA/TEOS/Ag-Np hybrid thin films, Journal of Colloid and Interface Science, 349, 2010, 77-85.
5. K. Vasilev, Nanoengineered Antibacterial Coatings and Materials: A Perspective, Coatings, 9, 2019, 654-666.
6. M.B. Ballatore, J. Durantini, N.S. Gsponer, M.B. Suarez, M. Gervaldo, L. Otero, M.B. Spesia, M.E. Milanesio, E.N. Durantini, Photodynamic inactivation of bacteria using novel electrogenerated porphyrin-fullerene C60 polymeric films, Environ. Sci. Technol., 49, 2015, 7456-63.
7. L. Brovko, H. Anany, M. Bayoumi, K. Giang, E. Kunkel, E. Lim, O. Naboka, S. Rahman, J. Li, C.D. M. Filipe, M.W. Griffiths, Antimicrobial Light-Activated Materials: Towards Application for Food and Environmental Safety, J. Appl. Microbiol. 117, 2014, 1260-1266.
8. A. Nyga, D. Czerwinska-Główka,́ M. Krzywiecki, W. Przystaś, E. Zabłocka-Godlewska, S. Student, M. Kwoka, P. Data, A. Blacha-Grzechnik, Covalent Immobilization of Organic Photosensitizers on the Glass Surface: Toward the Formation of the Light Activated Antimicrobial Nanocoating, Materials, 14, 2021, 3093.
9. E. Alves, M.A.F. Faustino, M.G.P.M.S. Neves, A. Cunha, J. Tome, A. Almeida, An insight on bacterial cellular targets of photodynamic inactivation. Fut. Med. Chem., 6, 2014, 141-164.
10. J. Bozja, J. Sherrill, S. Michielsen, I. Stojiljkovic, Porphyrin-based, light-activated antimicrobial materials. J. Polym. Sci., Part A: Polym. Chem., 41, 2003, 2297-2303.
11. M. Krouit, R. Granet and P. Krausz, Photobactericidal films from porphyrins grafted to alkylated cellulose – Synthesis and bactericidal properties, Eur. Polym. J., 45, 2009, 1250-1259.
12. I. Banerjee, R.C. Pangule and R.S. Kane, Antifouling coatings: recent developments in the design of surfaces that prevent fouling by proteins, bacteria, and marine organisms, Adv. Mater., 23, 2011, 690-718.
13. S.F. Musolino, F. Shatila, G.M. Tieman, A.C. Masarsky, M.C. Thibodeau, J.E. Wulff, H.L. Buckley,. Light-Induced Anti-Bacterial Effect Against Staphylococcus aureus of Porphyrin

Covalently Bonded to a Polyethylene Terephthalate Surface, ACS omega, 7, 2022, 29517-29525.
14. A. Charlot, V. Sciannamea, S. Lenoir, E. Faure, R. Jérôme, C. Jérôme, et al., All-in-one strategy for the fabrication of antimicrobial biomimetic films on stainless steel, Mater. Chem. 19, 2009, 4117-4125.
15. E. Faure, P. Lecomte, S. Lenoir, C. Vreuls, C. Van De Weerdt, C. Archambeau, et al. Sustainable and bio-inspired chemistry for robust antibacterial activity of stainless steel, J. Mater. Chem., 21, 2011, 7901-7904.
16. E. Faure, C. Falentin, T.C. Lanero, C. Vreuls, G. Zocchi, C. Van de Weerdt et al., Functional Nanogels as Platforms for Imparting Antibacterial, Antibiofilm, and Antiadhesion Activities to Stainless Steel, Adv. Funct. Mater., 22, 2012, 5271-5282.
17. Image-Pro® Plus Version 7.0 for Windows Start-Up Guide, Media Cybernetics, Inc., pp. 1-78.
18. N. Philipova, N. Mineva, R. Bryaskova, Surface and mechanical properties of bio-inspired coatings, Journal of Chemical Technology and Metallurgy, 56, 2021, 671-677.
19. R. Bryaskova, N. Philipova, N. Georgiev, I. Lalov, V. Bojinov, C. Detrembleur, Photoactive mussels inspired polymer coatings: Preparation and antibacterial activity, Journal of Applied Polymer Science, 138, 2021, 50769.
20. Y. Luan, H. Qi, N. Gao, G. Zheng, J. Wang, Synthesis of an amino-functionalized metal–organic framework at a nanoscale level for gold nanoparticle deposition and catalysis, Mater. Chem. A., 2, 2014, 20588-20596.
21. Y.-A.Li, S. Yang, Q.-K. Liu, G.-J. Chen, J.-P. Ma, Y.-B. Dong, Metal-Organic Framework Derived Carbons: Applications as Solid Base Catalyst and Support for Pd Nanoparticles in Tandem Catalysis, Chem. Commun. 52, 2016, 6517-6520.
22. S. Natarajan, G. Dutta, A.K. Jana, M. Eswaramoorthy, D.K. Singh, Encapsulation of Ag-nanoparticle in an amine – functionalized porphyrin MOF and its use as a heterogeneous catalyst for CO2 fixation under atmospheric pressure, Chem. Asian J., 13, 2018, 2677-2684.
23. Ch-S. Han, S.H.R. Sanei, F. Alisafaei, On the origin of indentation size effects and depth dependent mechanical properties of elastic polymers, Journal of Polymer Engineering, 36, 2016, 103-111.